Current Research in Food Science 7 (2023) 100646

Contents lists available at ScienceDirect

Current Research in Food Science

journal homepage: www.sciencedirect.com/journal/current-research-in-food-science

Trifuhalol A, a phlorotannin from the brown algae *Agarum cribrosum,* reduces adipogenesis of human primary adipocytes through Wnt/β-catenin and AMPK-dependent pathways

Aaron Taehwan Kim, Yeonhwa Park *

Department of Food Science, University of Massachusetts, Amherst, MA, 01003, USA

ARTICLE INFO

Handling Editor: Dr. Quancai Sun

Keywords:
Trifuhalol A
Anti-obesity
Human adipocytes
Wnt
AMPK

ABSTRACT

Trifuhalol A, a fucol-type phlorotannin, was extracted and identified from the brown algae *Agarum cribrosum*. The total yield and purity of trifuhalol A from *A. cribrosum* were 0.98% and 86%, respectively. Trifuhalol A at 22 and 44 μM inhibited lipid accumulation in human primary adipocytes. Consistently trifuhalol A suppressed the expression of adipogenesis-related genes, such as proliferator-activated receptor-gamma (PPAR-γ), CCAAT/enhancer-binding protein-alpha (C/EBP-α), fatty acid synthase (FAS), and sterol regulatory element-binding protein-1 (SREBP-1), in a dose-dependent manner. Trifuhalol A increased the level of proteins such as wingless/integrated (Wnt)10b, nuclear-β-catenin, total-β-catenin, phospho-AMP-activated protein kinase (*p*AMPK), and phospho-liver kinase B1 (*p*LKB1) as well as the expression of genes such as Wnt10b, Frizzled 1, and low-density lipoprotein receptor-related protein 6 (LRP6). Additionally, trifuhalol A decreased the expression of the glycogen synthase kinase-3beta (GSK3β) gene. These results suggest that trifuhalol A reduces fat accumulation in human adipocytes via the Wnt/β-catenin- and AMPK-dependent pathways.

1. Introduction

The brown algae *Agarum cribrosum* is utilized in the food and functional food industry since it is readily available due to its omnipresence in the amphi-Pacific area. *Agarum cribrosum* is reported to contain abundant bioactive compounds that could be commercialized for functional foods, cosmetic merchandise, and biomedical products (Park et al., 2012). It possesses various phytochemicals, such as fucoidans, phycocolloids, pigments, and phlorotannins. Among them, phlorotannin, a group of phenolic compounds constituted by phloroglucinol (1,3,5-trihydroxybenzene), was found to be rich in brown algae compared to other types of red or green algae (Kamiya et al., 2010). Phlorotannins are known for their anti-diabetic and anti-obesity capacities, making them a high-value group of polyphenols (Gheda et al., 2021). Over 150 identified structurally diverse phlorotannins exist, yet most *in vitro* and *in vivo* studies are done on phlorotannin-rich extracts (Venkatesan et al., 2019; El Boukhari et al., 2020). Many identified phlorotannins have yet to be readily available in purified forms due to the lack of commercial use or the difficulty of mass production by synthesis. Among them, trifuhalol A, a fucol-type phlorotannin, was previously purified from the brown algae *Agarum cribrosum* and reported to have anti-inflammatory and antioxidant activities in murine RAW264.7 cells (Phasanasophon and Kim, 2019). However, the anti-obesity effect of trifuhalol A has not been studied; thus, the current study aimed to determine the role of trifuhalol A, found in brown algae, in adipogenesis using human primary preadipocytes.

2. Materials and methods

2.1. Materials

Human preadipocytes and culture media were purchased from ZenBio, Inc. (Research Triangle Park, NC, USA). Rabbit immunoglobulin G (IgG) monoclonal antibodies against *p*AMPK, *p*LKB1, and β-catenin were purchased from Cell Signaling Technology (Danvers, MA, USA). Rabbit anti-Wnt10b, α-tubulin, and the secondary antibody (goat anti-rabbit IgG antibody conjugated to horseradish peroxidase) were purchased from Abcam (Waltham, MA, USA). Other chemicals were bought from Fisher Scientific (Pittsburgh, PA, USA) unless stated in the described methods.

* Corresponding author. Department of Food Science, University of Massachusetts, Amherst, MA, 01003, USA.
E-mail address: ypark@umass.edu (Y. Park).

https://doi.org/10.1016/j.crfs.2023.100646
Received 6 October 2023; Received in revised form 8 November 2023; Accepted 15 November 2023
Available online 22 November 2023

2.2. Preparation of sample

Brown algae, *Agarum cribrosum*, collected in the ocean east of Gangneung, Republic of Korea in March 2020, were purchased from the Gangneung market. Sand, epiphytes, and salt were removed by washing with water. Algae were then air-dried for 7 days. The dried brown algae were ground with two consecutive grinders (LBC 15; Waring Commercial, Torrington, CT, USA, and HMF-3000S; Hanil, Seoul, Republic of Korea) and sieved through 300 μm. The dried powder was stored in sealed bags at −80 °C.

The extraction was carried out according to the method of Deenu et al. (2013) with a slight modification. The brown algae powder was mixed with 70% acetone with a 1 g to 35 mL ratio and extracted with an ultrasonic generator (Flexonic-500; Mirae Ultrasound Technology, Bucheon, Republic of Korea). The extraction condition was as follows: intensity of 36.58 W/cm^2, frequency of 35 kHz, temperature of 30 °C, and time of 5.75 h. Then, the solution was centrifuged at 4500×*g* for 20 min, filtered through Whatman filter paper No. 1 (GE Healthcare Life Sciences, Chicago, IL, USA), and concentrated *in vacuo* at 37 °C. Phlorotannin was purified according to the modified method of Gall et al. (2015). Solvent fractionation was carried out in the sequential order of n-hexane, dichloromethane, ethyl acetate, and water. Each solvent and aqueous fraction were concentrated *in vacuo* at 37 °C and then freeze-dried. The ethyl acetate fraction was purified with Sephadex LH-20 column chromatography (GE Healthcare Life Sciences, Chicago, IL, USA). The six running eluents were as follows: water: methanol solution (1:1, 1:3 & 0:1) to methanol: acetone solution (5:1, 3:1 & 1:1), in order. Each elute was named as subfractions 1 to 6. All subfractions were concentrated *in vacuo* at 37 °C, lyophilized, and stored at −80 °C. The yield of the crude extract was calculated as (weight of crude extract/-weight of algae powder) × 100. The yield of the solvent fractionation was calculated as (weight of partitioned fraction/weight of crude extract) × 100. The yield of the column chromatography was calculated as (weight of Sephadex subfraction/weight of ethyl acetate fraction injected into the column) × 100.

2.3. Determination of total phlorotannin content

The total phlorotannin content was determined according to the method of Singleton and Rossi (1965). The standard was 98% phloroglucinol (PGE, 50–300 μg/mL) from Thermo Fisher Scientific (Waltham, MA, USA). A mixture of 200 μL of subfraction sample, 2.6 mL distilled water, and 200 μL of 2 M Folin-Ciocalteu reagent were incubated at room temperature for 6 min. The reaction was stopped by adding 2 mL of 7% (w/v) Na_2CO_3. The mixture was incubated again at room temperature for 90 min, and the absorbance at 750 nm was measured with a UV-VIS Spectrophotometer (V-530; Jasco, Tokyo, Japan). Total phlorotannin content was calculated from the regression equation of the standard curve from phloroglucinol.

2.4. High-performance liquid chromatography with diode-array detection and quality management system analysis

The purified phlorotannin sample was analyzed by High-Performance Liquid Chromatography (HPLC) (Agilent 1100 series; Agilent Technologies Inc., Santa Clara, CA, USA) equipped with an autosampler/injector, a column compartment, a binary pump, and a diode array detector. The column was a Zorbax Analytical Rx-C18 (4.6 × 250 mm, 5 μm, Agilent Technologies Inc.). The flow rate was 1 mL/min. A mobile phase was 0.1% formic acid in aqueous solution, and B was 0.1% formic acid in acetonitrile. The linear gradient was as follows: 0–8 min (5–15% B), 8–10 min (15–30% B), 10–18 min (30–35% B), 18–23 min (35–100% B), 23–35 min (100% B), and 35–40 min (100–5% B). A wavelength at 280 nm was recorded. Mass spectrometric analysis (Agilent 6120; Agilent Technologies Inc., Santa Clara, CA, USA) was performed. Qualitative analysis was done by LC/MSC Chem Station B.04.03 software (Agilent Technologies Inc. address, Santa Clara, CA, USA).

2.5. Cell culture

The culture and differentiation of human primary preadipocytes were followed by the manufacturer's manual (ZenBio Inc., Triangle Park, NC, USA). Briefly, the deep-frozen cell vial was thawed at 37 °C water bath upon arrival and cultured with preadipocyte medium at 37 °C in a humidified 5% CO_2 atmosphere. The medium was changed every other day until the cell confluency reached 90%. The medium was changed to differentiation medium, and the day was designated as day 1. Different concentrations of trifuhalol A were treated on day 1. The new differentiation medium containing trifuhalol A was changed every other day until cells were harvested on day 15. Cell viability was determined using an Ez-cytox cell viability assay kit (DoGenBio, Seoul, Republic of Korea). The absorbance at 450 nm was measured using a microplate reader (EL-800; BioTek, Winooski, VT, USA).

2.6. Determination of accumulated fat

Oil-Red-O staining and triglyceride quantification were used to determine the accumulated fat from cells, followed by the method of Gunasinghe et al. (2019). Cells were observed with a Moticam Digital Color Camera (Ted Pella Inc., Redding, CA, USA). Cells were lysed with 100% isopropanol, and the absorbance at 490 nm was measured. Triglyceride analysis was determined using a Triglyceride Quantification Kit (BioVision, Mountain View, CA, USA). The absorbance at 570 nm was measured using a spectrophotometer (Biotek, Winooski, VT, USA).

2.7. Real-time polymerase chain reaction

Tri reagent® (Molecular Research Center Inc., Cincinnati, OH, USA) was used to extract RNA from each well. The concentration of the extracted RNA was analyzed with a nanophotometer (P330; Implen GmbH, Munich, Germany). High Capacity cDNA Reverse Transcription kit (Applied Biosystems, Foster City, CA, USA) was used to synthesize cDNA from extracted RNA. Quantification of gene expression was performed using the QuantStudio™ 7 FlexReal-Time PCR System (Thermo Fisher Scientific, Waltham, MA, USA) and SYBR® Premix EX Taq™ II (Takara Bio Inc., Kusatsu, Shiga, Japan). Relative gene expression was calculated using the $2_T^{-\Delta\Delta C}$ method (Livak and Schmittgen, 2001). Primer sequences were assessed from the National Center for Biotechnology Information (Bethesda, MD, USA) and analyzed with OligoAnalyzer (Integrated DNA Technologies, Coralville, IA, USA). Forward and reverse sequences of tested genes are listed in Supplementary Table S1.

2.8. Western blot analysis

Radioimmunoprecipitation assay buffer (T&I, Seoul, Republic of Korea) containing protease inhibitor cocktail (T&I) was used to extract proteins, which were quantified using a Pierce BCA Protein Assay kit (Thermo Fisher Scientific, Waltham, MA, USA). Thirty micrograms/lane of proteins went through 10% sodium dodecyl sulfate-polyacrylamide gel electrophoresis and transferred to polyvinylidene fluoride membranes. Membranes were blocked using 5% non-fat skim milk in tris-buffered saline containing Tween 20 (TBST) at room temperature for 1 h. Membranes were incubated again with primary antibodies: nuclear-β-catenin (1:1000), total-β-catenin (1:1000), Wnt10b (1:500), and β-actin (1:1000). Then, another 1hr incubation was followed with the secondary antibody (1:1000). Triple rinsing with TBST was performed between each and after incubations. ECL Advanced Western blotting detection reagent (Thermo Fisher Scientific, Waltham, MA, USA) was used to visualize targeted proteins. ChemiDoc XRS+ with Image Lab Software (Bio-Rad Laboratories, Hercules, CA, USA) was used to analyze proteins.

2.9. Statistical analysis

All experiments were carried out in triplicates, and all data were present as mean ± standard errors. Statistical analysis was performed using SPSS 23.0 (SPSS Inc., Chicago, IL, USA). Differences between groups were assessed by one-way analysis of variance followed by Tukey's multiple-range test. Differences between groups were considered to be statistically significant at $p < 0.05$.

3. Results and discussion

3.1. Characteristics of trifuhalol A from A. cribrosum

The phytochemicals from the brown algae *Agarum cribrosum* powder were extracted by ultrasonication, which is known to have increased yield through the bubble cavitation process compared to the conventional solvent extraction method (Ummat et al., 2020). According to Fig. 1, the ultrasound extraction yielded 9.0% with a total phlorotannin content value of 18.27 mg phloroglucinol equivalent (PGE)/g of sample. After the sequential solvent fractionation, the ethyl acetate fraction had the highest total phlorotannin content of 57.50 mg PGE/g with a yield of 13.8% (Fig. 1). Subsequently, the ethyl acetate extract was separated further by Sephadex LH-20 chromatography, resulting in subfractions 5 and 6 having total phlorotannin content of 67.24 and 69.68 mg PGE/g with yields of 25.6 and 53.4%, respectively (Fig. 1). Subfraction 4 displayed the highest total phlorotannin content of 48.70 mg PGE/g, yet the yield was considerably lower than subfractions 5 and 6 (Fig. 1). Therefore, subfractions 5 and 6 were selected for further HPLC-DAD-QMS analysis, which contained a peak at the same retention time with a purity of up to 86% (Fig. 2A and B). Mass spectrometry revealed the molecular ions at *m/z* $[M+H]^+$ 391.0, $[M+Na]^+$ 413.1, and $[2M+M]^+$ 803.1 (Fig. 2C). Based on the previous report (Le Lann et al., 2016), the molecular mass was determined as 390 Da. To further analyze the structure, nuclear magnetic resonance (NMR) analysis was followed (Fig. S1). The NMR data displayed the resonance at δ_H 5.89–6.3 and δ_C 95–163 ppm, which were the characteristics of phlorotannin (Le Lann et al., 2016). ^{1}H-NMR spectra showed three characteristics of aromatic ^{1}H: 5.89, 5.90, and 5.92 ppm. ^{13}C-NMR spectrum was used to determine the types of linkage: C-O-C linkage from 125.13, 125.78, 158.67, and 158.80 ppm; C-H linkage from 95.54 to 98.10 ppm; C-OH linkages from 147.99, 152.46, 152.60 and 152.68 ppm; phenolic C from 152 to 159 ppm (Supplementary Figure S1). The vacancy at 100–105 spectrum explained the absence of aryl-aryl C. Based on the described data and the previous publication, the compound was identified as trifuhalol A, a type of phlorotannin (Phasanasophon and Kim, 2017).

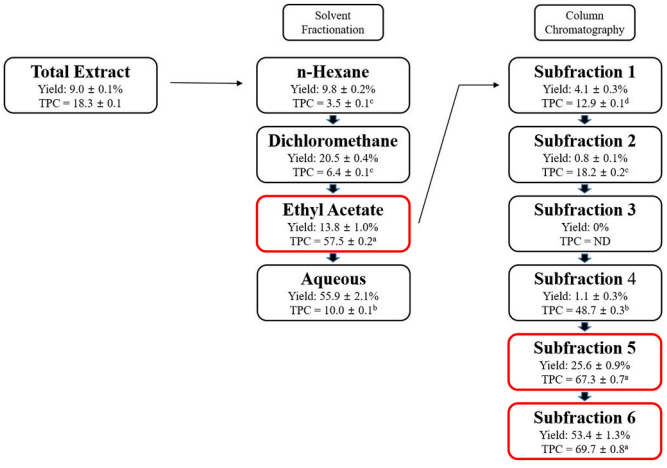

Fig. 1. Yields and total phlorotannin content of the extract, solvent fractions, and subfractions from ethyl acetate fraction of *A. cribrosum*. Yield and total phlorotannin contents (TPC) were determined from 3 independent experiments. TPC, total phlorotannin content (mg of phloroglucinol equivalent/g of sample); ND, Not Detected. [a-d]Different letters indicate significant difference within the same purification step ($p < 0.05$).

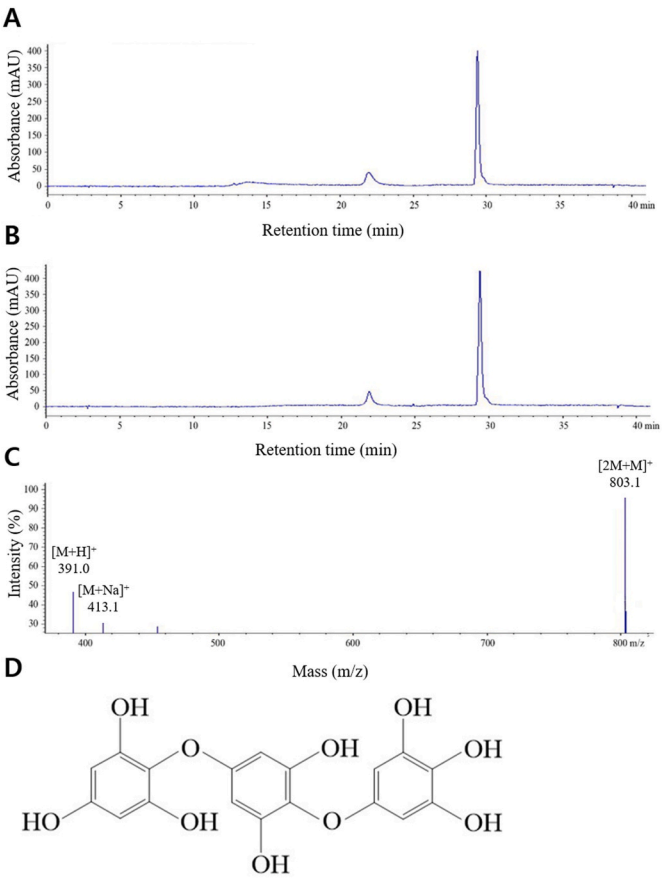

Fig. 2. Purity of fractions and structure of trifuhalol A. (A) HPLC chromatogram of subfraction 5 and (B) subfraction 6. (C) Mass spectra of subfractions 5 + 6. (D) Structure of trifuhalol A.

3.2. Cytotoxicity of trifuhalol A on human adipocytes

Previously, phlorotannins were reported to have no significant toxicity up to 1500 mg/kg in mice and 263 mg/day in humans (Nagayama et al., 2002; Turch et al., 2017). However, the toxicity of phlorotannins was observed in human and rat leukemia cells at a relatively high concentration of 500 μM (Le et al., 2009). Thus, we determined the cytotoxicity of trifuhalol A from *A. cribrosum* in human primary preadipocytes using 10–160 μg/mL extract, which is equivalent to 22–352 μM based on purity of 86% in subfractions 5 & 6. The concentration of 22 μM and 44 μM of trifuhalol A did not show cytotoxicity when treated for 15 days of adipogenesis (Fig. 3). However, we observed significant cytotoxicity with a concentration higher than 88 μM of trifuhalol A on day 15 (Fig. 3). At 176 μM and 352 μM of trifuhalol A significantly decreased the cell viability by 33% and 51% on day 15 compared to the control, respectively (Fig. 3). Therefore, we used 22 μM and 44 μM of trifuhalol A for the following experiments.

3.3. Reduced fat accumulation by trifuhalol A

Trifuhalol A was tested for its role in fat accumulation using Oil-Red-O staining and quantifying the triglyceride contents in the mature human adipocytes (Fig. 4). Undifferentiated human preadipocytes showed no to minimum stain by Oil-Red-O and triglyceride contents,

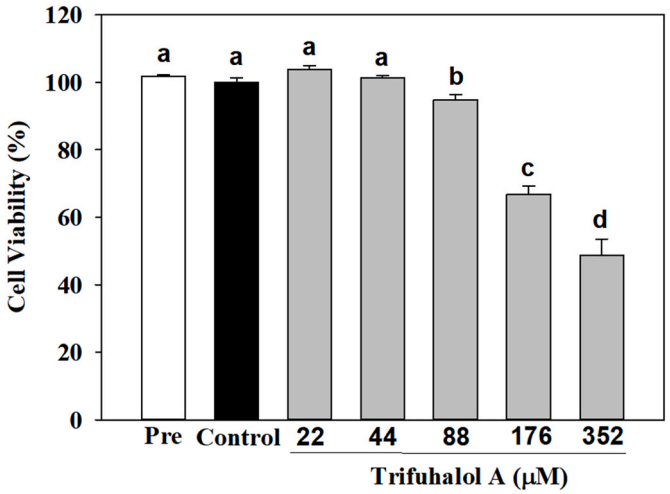

Fig. 3. Effects of trifuhalol A from *A. cribrosum* on cell viability of human primary preadipocytes and adipocytes. Cells were treated with trifuhalol A from day 0 to day 15 of adipocytic differentiation. Data are shown as mean ± standard error (n = 3). Means with different letters are significantly different at $p < 0.05$. Pre, Human preadipocytes; Control, Human adipocytes.

whereas, in mature adipocytes, trifuhalol A inhibited the accumulation of lipid and triglyceride in a dose-dependent manner compared to the fully matured adipocyte control (Fig. 4). Treatment of trifuhalol A at 44 μM suppressed lipid accumulation by ~16% compared to the control (Fig. 4B and C). Previously, several phlorotannins were reported to suppress lipid accumulation *in vitro* as well as *in vivo,* such as in mice and zebrafish (Choi et al., 2015), but the current work would be the first to report the reduced fat accumulation of a phlorotannin in human adipocytes.

Real-time PCR analysis was followed to determine the role of trifuhalol A in key adipogenesis-related genes. Peroxisome proliferator-activated receptor-gamma (PPAR-γ) and CCAAT/enhancer-binding protein-alpha (C/EBP-α) are key transcription factors of adipogenesis and activate expressions of down-stream genes involved in adipogenesis (Dunning et al., 2014; Ye et al., 2017; Zhang et al., 2018). Treating cells with trifuhalol A at 22 and 44 μM was able to suppress the expression of PPAR-γ by 18% and 26%, and C/EBP-α by 21% and 31% compared to the controls, respectively (Fig. 5A and B). In addition, fatty acid synthase (FAS) and sterol regulatory element-binding protein-1 (SREBP1) are involved in lipogenesis, particularly in converting carbohydrates to fatty acids (Hwang et al., 2017). Treatment of trifuhalol A at 22 and 44 μM inhibited FAS by 13% and 28%, and SREBP1 by 13% and 39% compared to the controls, respectively (Fig. 5C and D). These results support that trifuhalol A reduced fat accumulation by inhibiting the expression of adipogenic transcription factors and their downstream genes.

3.4. Inhibition by trifuhalol A on adipogenesis pathways

The Wnt signaling is an important pathway in cellular homeostasis and differentiation and functions via two distinct pathways: β-catenin-dependent canonical pathway (Wnt/β-catenin) and β-catenin-independent non-canonical pathways (Wnt/Ca^{2+} and planar cell polarity; PCP) (Song and Wang, 2020). The canonical Wnt/β-catenin pathway is vital in cell differentiation, survival, growth, and proliferation, whereas the non-canonical Wnt pathway controls cell migration and polarity (Fan et al., 2017; Liu et al., 2022). With regards to adipocyte differentiation, it is known that the canonical Wnt/β-catenin pathway suppresses adipogenesis by blocking C/EBPα and PPARγ, whereas the non-canonical Wnt pathway acts as pro-adipogenic by antagonizing the canonical Wnt pathway (Christodoulides et al., 2009; van Tienen et al., 2009).

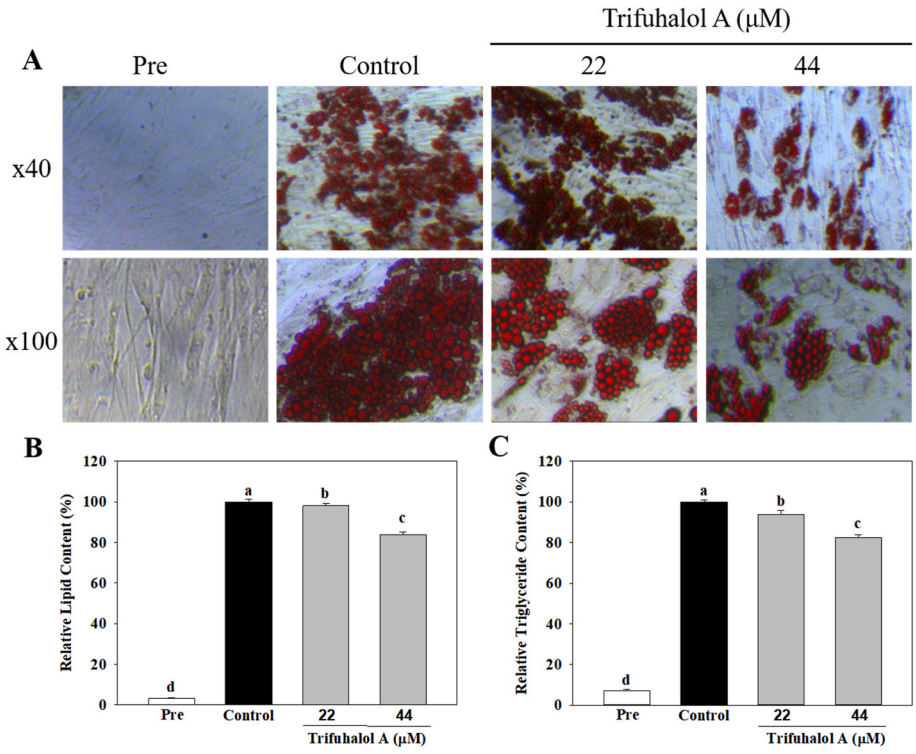

Fig. 4. Effects of trifuhalol A from *A. cribrosum* on lipid accumulation in human adipocytes. (A) Representation of Oil-Red-O staining of differentiated human adipocytes at magnification of 40 and 100. (B) Quantification of Oil-Red-O stained differentiated human adipocytes. (C) Relative triglyceride content of differentiated human adipocytes. Cells were treated with trifuhalol A for 15 days. Data are shown as the mean ± standard error (n = 3). Means with different letters indicate significant differences at $p < 0.05$. Pre, Human preadipocytes; Control, Human adipocytes. (For interpretation of the references to colour in this figure legend, the reader is referred to the Web version of this article.)

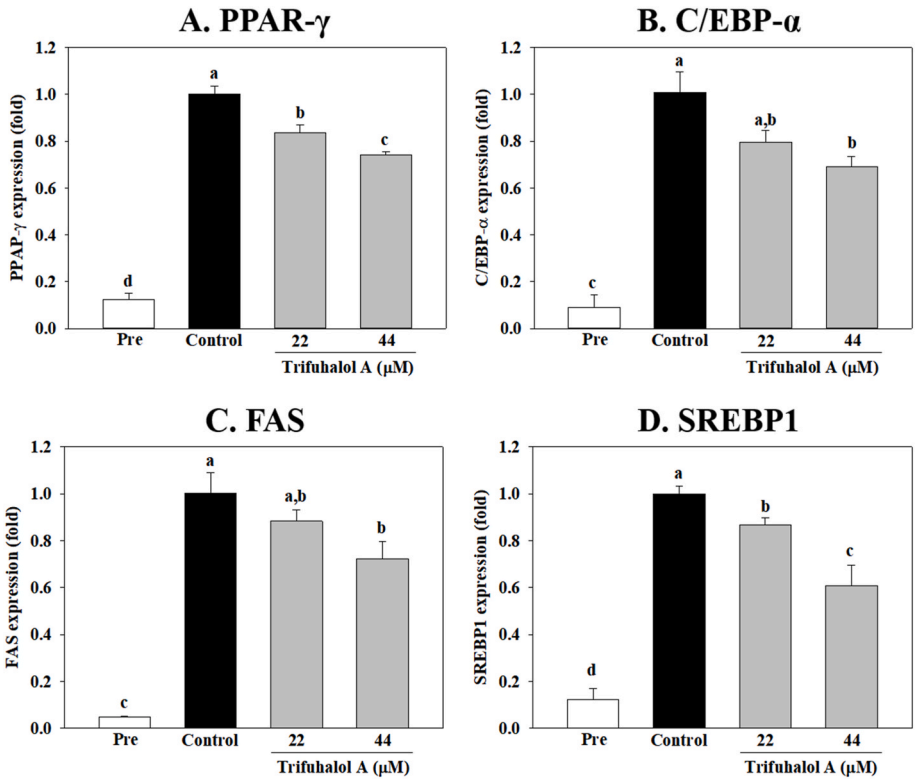

Fig. 5. Effects of trifuhalol A from *A. cribrosum* on adipogenesis-related gene expression. (A) Proliferator-activated receptor-gamma (PPAR-γ), (B) CCAAT/Enhancer-binding protein-alpha (C/EBP-α), (C) Fatty acid synthase (FAS), and (D) Sterol regulatory element-binding protein-1 (SREBP1). Cells were treated with trifuhalol A for 15 days. Data are shown as the mean ± standard error (n = 3). Means with different letters indicate significant differences at $p < 0.05$. Pre, Human preadipocytes; Control, Human adipocytes.

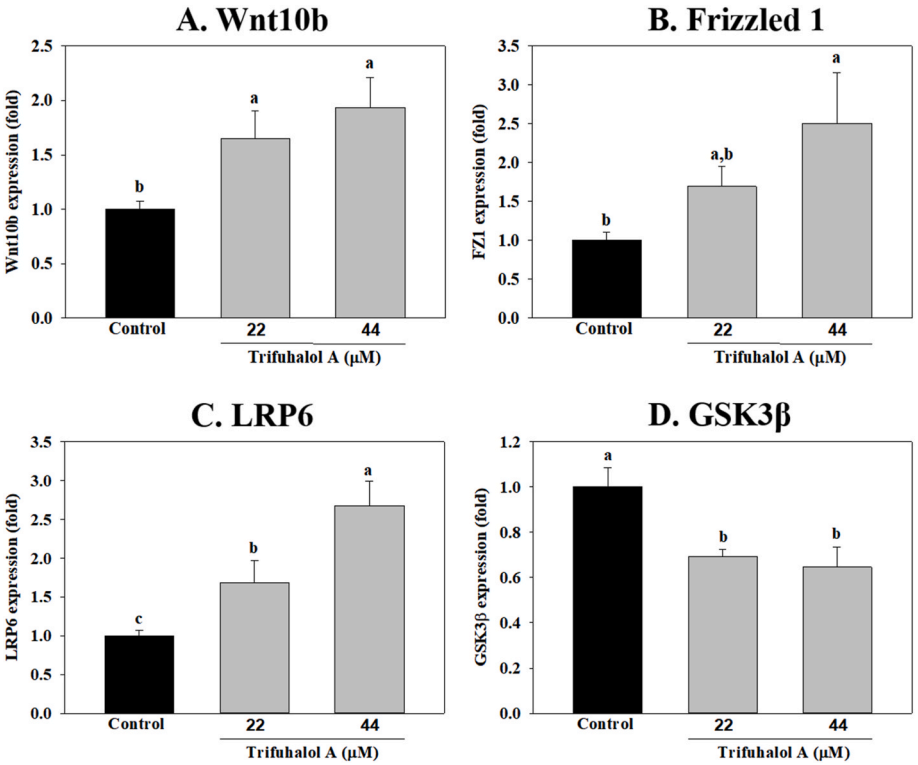

Fig. 6. Effects of trifuhalol A from *A. cribrosum* on pathway-related genes. (A) Wnt Family member 10b (Wnt10b), (B) Frizzled 1, (C) Lipoprotein receptor-related protein 6 (LRP6) and (D) Glycogen synthase kinase 3 beta (GSK3β). Cells were treated with trifuhalol A for 15 days. Data are shown as the mean ± standard error (n = 3). Means with different letters indicate significant differences at $p < 0.05$.

However, with its high complexity due to the diversity and interplay of receptors and co-receptors, the importance of the non-canonical Wnt pathway during adipogenesis *in vivo* remains less established (Fuster et al., 2015). Thus, we focused on whether trifuhalol A acts via the canonical Wnt/β-catenin signaling pathway in human adipocytes.

When the canonical Wnt pathway is not activated, the destruction complex (composed of glycogen synthase kinase 3 beta, GSK3β, axin, adenomatous polyposis coli, casein kinase-1, and β-transducin) remains active, and GSK3β phosphorylates β-catenin leading to degradation of β-catenin (Pakula et al., 2017). The canonical Wnt pathway is activated when frizzled 1 or its co-receptor lipoprotein receptor-related protein (LRP) 5/6 binds with one of the canonical Wnt ligands (such as Wnt family member 1, 3a, and 10b; Wnt1, Wnt3a, Wnt10b), leading to inhibition of the destruction complex; thus, β-catenin enters the nucleus to start transcription of downstream genes (Wang et al., 2020). In this study, we examined the effects of trifuhalol A in canonical Wnt/β-catenin signaling pathway: Wnt family member 10b (Wnt10b), frizzled 1, LRP 6 and GSK-3β. Treatment of trifuhalol A significantly increased levels of Wnt10b, frizzled 1, and LRP6 compared to the control in a dose-dependent manner (Fig. 6A–C). In addition, trifuhalol A suppressed the expression of GSK-3β, which was overexpressed during adipogenesis (Fig. 6D). These were further confirmed by the Western blot analysis that trifuhalol A increased protein levels of Wnt10b, nuclear-β-catenin, and total-β-catenin compared to the control (Fig. 7A–D). These results suggest that trifuhalol A may target the Wnt/β-catenin signaling pathway to reduce fat accumulation in this model.

Additionally, we examined *p*AMPK and *p*LKB1 proteins, which are key elements in the AMPK signaling pathway. Phosphorylated LKB1 protein induces phosphorylated AMPK, which inhibits lipogenesis. In addition, the AMPK pathway is reported to interplay with the canonical Wnt/β-catenin pathway (Zhao et al., 2010), and GSK-3β is inhibited by the AMPK pathway (Wang et al., 2020). Our results showed that trifuhalol A increased the levels of *p*AMPK and *p*LKB1 (Fig. 7E and F). Therefore, the anti-obesity aspects of trifuhalol A act in part via the Wnt/β-catenin as well as AMPK signaling pathways.

There are previous reports of the anti-obesity effects of various phlorotannins using isolates or extracts: Kim et al. (2013) previously reported anti-adipogenic effect of phlorotannin-rich methanol extract of *Ecklonia cava* on 3T3-L1 adipocytes dependent on PPAR-γ. Consistently, five phlorotannins (dieckol, dioxinodehydroeckol, dieckol, phlorofucofuroeckol A, and phloroglucinol) from *Ecklonia stolonifera* displayed anti-adipogenic activity on 3T3-L1 through C/EBPα and PPARγ (Jung et al., 2014). Another study reported phlorotannin derivatives (triphlorethol-A, eckol, and dieckol) suppressed adipogenesis via SREBP1c, C/EBPα, and PPARγ in 3T3-L1 adipocytes (Karadeniz et al., 2015). In addition, there are limited *in vivo* studies with phlorotannins; dieckol from *E. cava* inhibited fat accumulation in high-fat diet zebrafish and mice through AMPKα signaling pathways (Choi et al., 2015). Various phlorotannins from brown algae displayed anti-obesity aspects in different experimental models, but more studies should be followed to understand the role of phlorotannins in adipogenesis further.

Phlorotannins from brown algae with various concentrations (1–200 μM; 60–2000 mg/kg body weight) displayed little to no significant toxicity in different cell lines, plants, microalgae, invertebrates, and animals (zebrafish, mice, rats, dogs), while expressing some health beneficial effects, such as tumor suppression, or reduced lipid accumulation (Negara et al., 2021). Although limited, clinical studies with phlorotannins or crude extracts reported no side effects or serious adverse effects with concentrations between 72 and 500 mg/capsule with 1–2 capsules/day up to 12 weeks (Paradis et al., 2011; Shin et al., 2012; Um et al., 2018). Additionally, previous studies mainly used the concentration range between 10 and 100 μM with minimum cytotoxicity, and clinical studies on phlorotannins extract from *E. cava* did not show adverse effects on patients with hypercholesterolemia or pre-diabetic conditions (Choi et al., 2015; Lee and Jeon, 2015). However, many studies use crude extracts, popular phlorotannins, such as eckol or dieckol, or common sources, such as *E. cava*. Other types of phlorotannins, such as trifuhalol A, have not been tested in animals or clinical trials.

Currently, only limited biological functions of trifuhalol A have been reported: Anti-inflammatory activities on murine RAW264.7 cells and anti-allergic effects in mice (Phasanasophon and Kim, 2019; Bong et al.,

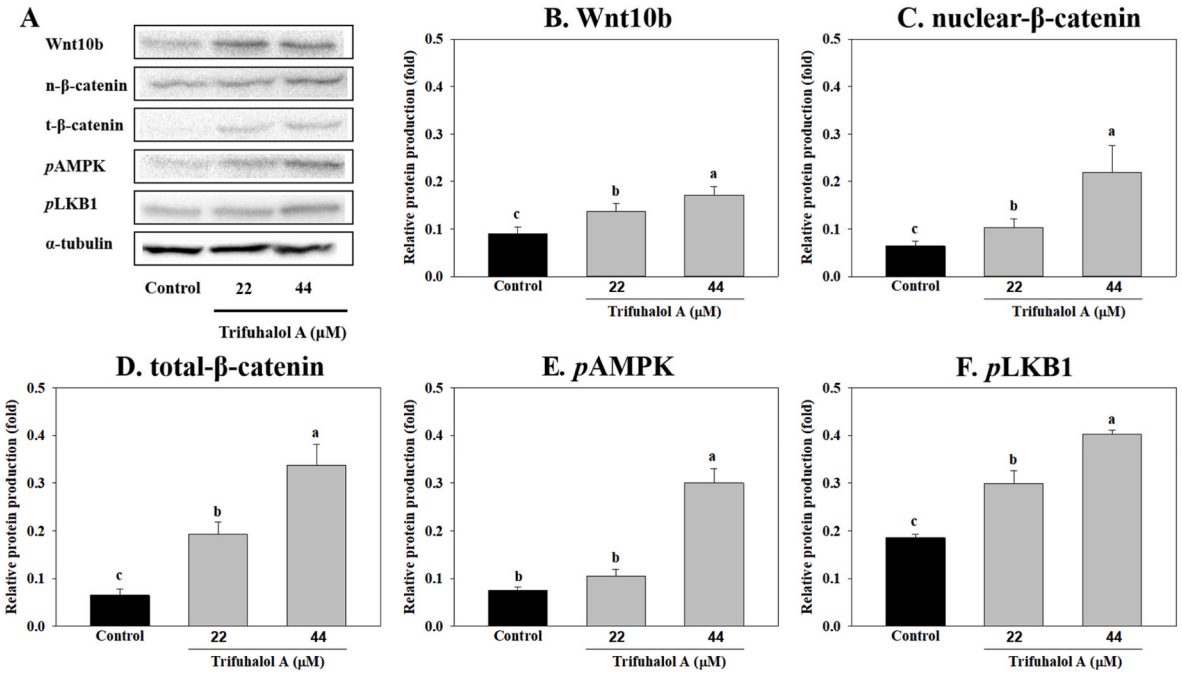

Fig. 7. Effects of trifuhalol A from *A. cribrosum* on production of various proteins in Wnt/β-catenin and AMPK pathway. Cells were treated with trifuhalol A for 15 days. (A) Western blot analysis with human adipocytes. Protein Quantification normalized by α-tubulin of (B) Wnt10b, (C) nuclear-β-catenin, (D) total-β-catenin, (E) phosphorylated AMPK, and (F) phosphorylated LKB1. Data are shown as the mean ± standard error (n = 3). Means with different letters indicate significant differences at $p < 0.05$.

2022). Therefore, this study would be the first to report reduced adipogenesis by trifuhalol A from brown algae *Agarum cribrosum*. The exact mechanisms of anti-obesity effects of phlorotannin are still limited and largely unknown, including the effects of trifuhalol A from *in vivo* models. However, based on previous reports that various types of phlorotannins, such as phloroglucinols and dieckol, displayed anti-obesity effects from both *in vitro* and *in vivo* studies (Choi et al., 2015; Ko et al., 2013; Lee and Jeon, 2015; Yoon et al., 2017), we expect that similar anti-obesity effects by trifuhalol A from *in vivo* studies. Therefore, more research should be followed to examine the potential significance of the current observations using *in vivo* models.

4. Conclusion

Trifuhalol A was purified from the brown algae *Agarum cribrosum* with a yield of 0.93% and a purity of 86%. Trifuhalol A inhibited lipid accumulation during adipogenesis by down-regulating the expression of adipogenesis-related genes in human primary adipocytes. The effects of trifuhalol A on fat accumulation depended on its role in the Wnt/β-catenin and AMPK pathways. Therefore, trifuhalol A from the brown algae could potentially be used for controlling adipogenesis.

CRediT authorship contribution statement

Aaron Taehwan Kim: Conceptualization, Data collection, Visualization, Writing. **Yeonhwa Park:** Conceptualization, Project administration, Supervision, Writing.

Declaration of competing interest

The authors declare the following financial interests/personal relationships which may be considered as potential competing interests: Given her role as the Associate Editor at the time of submission, Dr. Yeonhwa Park was not involved in the peer review of this article and had no access to information regarding its peer review. Full responsibility for the editorial process for this article was delegated to another editor, as per the Journal guidelines. The authors declare that they have no other known competing financial interests that could have appeared to influence the work reported in this paper.

Data availability

Data will be made available on request.

Acknowledgment

This project is partly supported by the F. J. Francis Endowment at the Department of Food Science, University of Massachusetts Amherst.

Appendix A. Supplementary data

Supplementary data to this article can be found online at https://doi.org/10.1016/j.crfs.2023.100646.

References

Bong, S.K., Park, N.J., Lee, S.H., Lee, J.W., Kim, A.T., Liu, X., Kim, S.M., Yang, M.H., Kim, Y.K., Kim, S.N., 2022. Trifuhalol A suppresses allergic inflammation through dual inhibition of TAK1 and MK2 mediated by IgE and IL-33. Int. J. Mol. Sci. 23 (17), 10163.

Choi, E.-K., Park, S.-H., Ha, K.-C., Noh, S.-O., Jung, S.-J., Chae, H.-J., Chase, S.-W., Park, T.-S., 2015. Clinical trial of the hypolipidemic effects of a brown alga *Ecklonia cava* extract in patients with hypercholesterolemia. Int. J. Pharmacol. 11 (7), 798–805.

Choi, H.-S., Jeon, H.-J., Lee, O.-H., Lee, B.-Y., 2015. Dieckol, a major phlorotannin in *Ecklonia cava* suppresses lipid accumulation in the adipocytes of high-fat diet-fed zebrafish and mice: inhibition of early adipogenesis via cell-cycle arrest and AMPKα activation. Mol. Nutr. Food Res. 59 (8), 1458–1471.

Christodoulides, C., Lagathu, C., Sethi, J.K., Vidal-Puig, A., 2009. Adipogenesis and wnt signalling. TEM (Trends Endocrinol. Metab.) 20 (1), 16–24.

Deenu, A., Naruenartwongsakul, S., Kim, S.M., 2013. Optimization and economic evaluation of ultrasound extraction of lutein from *Chlorella vulgaris*. Biotechnol. Bioproc. Eng. 18, 1151–1162.

Dunning, K.R., Anastasi, M.R., Zhang, V.J., Russell, D.L., Robker, R.L., 2014. Regulation of fatty acid oxidation in mouse cumulus-oocyte complexes during maturation and modulation by RRAG agonists. PLoS One 9 (2), e87327.

El Boukhari, M.E.M., Barakate, M., Bouhia, Y., Lyamlouli, K., 2020. Trends in seaweed extract based biostimulants: manufacturing process and beneficial effect on soil-plant system. Plants 9 (3), 359.

Fan, J., Wei, Q., Liao, J., Zou, Y., Song, D., Xiong, D., Ma, C., Hu, X., Qu, X., Chen, L., Li, L., Yu, Y., Yu, X., Zhang, Z., Zhao, C., Zeng, Z., Zhang, R., Yan, S., Wu, T., Wu, X., Shu, Y., Lei, J., Li, Y., Zhang, W., Haydon, R.C., Luu, H.H., Huang, A., He, T.-C., Tang, H., 2017. NoncanonicalWnt signaling plays an important role in modulating canonical Wnt-regulated stemness, proliferation and terminal differentiation of hepatic progenitors. Oncotarget 8 (16), 27105–27119.

Fuster, J.J., Zuriaga, M.A., Ngo, D.T., Farb, M.G., Aprahamian, T., Yamaguchi, T.P., et al., 2015. Noncanonical wnt signaling promotes obesity-induced adipose tissue inflammation and metabolic dysfunction independent of adipose tissue expansion. Diabetes 64, 1235–1248.

Gall, E.A., Lelchat, F., Hupel, M., Jégou, C., Stiger-Pouvreau, V., 2015. Extraction and purification of phlorannins from brown algae. In natural products from marine algae. Methods Mol. Biol. 1308, 131–143.

Gheda, S., Naby, M.A., Mohamed, T., Pereira, L., Khamis, A., 2021. Antidiabetic and antioxidant activity of phlorotannins extracted from the brown seaweed *Cystoseira compressa* in streptozotocin-induced diabetic rats. Environ. Sci. Pollut. Res. Int. 28 (18), 22886–22901.

Gunasinghe, M.A., Kim, A.T., Kim, S.M., 2019. Inhibitory effects of vanadium-binding proteins purified from the sea squirt *Halocynthia roretzi* on adipogenesis in 3T3-L1 adipocytes. Appl. Biochem. Biotechnol. 189, 49–64.

Hwang, D., Won, K., Kim, D., Kim, B., Lee, H.M., 2017. Cinnamyl alcohol, the bioactive component of chestnut flower absolute, inhibits adipocyte differentiation in 3T3-L1 cells by downregulating adipogenic transcription factors. Am. J. Chin. Med. 45, 833–846.

Jung, H.A., Jung, H.J., Jeong, H., Kwon, H.J., Ali, M.Y., Choi, J.S., 2014. Phlorotannins isolated from the edible brown alga *Ecklonia stolonifera* exert anti-adipogenic activity on 3T3-L1 adipocytes by downregulating C/EBPα and PPARγ. Fitoterapia 92, 260–269.

Kamiya, M., Nishio, T., Yokoyama, A., Yatsuya, K., Nishigaki, T., Yoshikawa, S., Ohki, K., 2010. Seasonal variation of phlorotannin in sargassacean species from the coast of the Sea of Japan. Phycol. Res. 58 (10), 53–61.

Karadeniz, F., Ahn, B.N., Kim, J.A., Seo, Y., Jang, M.S., Nam, K.H., Kim, M., Lee, S.H., Kong, C.S., 2015. Phlorotannins suppress adipogenesis in pre-adipocytes while enhancing osteoblastogenesis in pre-osteoblasts. Arch Pharm. Res. (Seoul) 38, 2172–2182.

Kim, H., Kong, C.S., Lee, J.I., Kim, H., Baek, S., Seo, Y., 2013. Evaluation of inhibitory effect of phlorotannins from *Ecklonia cava* on triglyceride accumulation in adipocyte. J. Agric. Food Chem. 61, 8541–8547.

Ko, S.-C., Lee, M., Lee, J.-H., Lee, S.-H., Lim, Y., Jeon, Y.-J., 2013. Dieckol, a phlorotannin isolated from a brown seaweed, *Ecklonia cava*, inhibits adipogenesis through AMP-activated protein kinase (AMPK) activation in 3T3-L1 preadipocytes. Environ. Toxicol. Pharmacol. 36 (3), 1253–1260.

Lee, S.-H., Jeon, Y.-J., 2015. Efficacy and safety of a dieckol-rich extract (AG-dieckol) of brown algae, *Eckonia cava*, in pre-diabetic individuals: a double-blind, randomized, placebo-controlled clinical trial. Food Funct. 6 (3), 853–858.

Le, Q.T., Li, Y., Qian, Z.J., Kim, M.M., Kim, S.K., 2009. Inhibitory effects of polyphenols isolated from marine alga *Ecklonia cava* on histamine release. Process Biochem. 44, 168–176.

Le Lann, K., Surget, G., Couteau, C., Coiffard, L., Cérantola, S., Gaillard, F., Larnicol, M., Zubia, M., Guérard, F., Poupart, N., Stiger-Pouvreau, V., 2016. Sunscreen, antioxidant, and bactericide capacities of phlorotannins from the brown macroalga *Halidrys siliquosa*. J. Appl. Phycol. 28, 3547–3559.

Liu, J., Xiao, Q., Xiao, J., Niu, C., Li, Y., Zhang, X., Zhou, Z., Shu, G., Yin, G., 2022. Wnt/β-catenin signaling: function, biological mechanisms, and therapeutic opportunities. Signal Transduct. Targeted Ther. 7, 3.

Livak, K.J., Schmittgen, T.D., 2001. Analysis of relative gene expression data using real-time quantitative PCR and the 2(-delta delta C(T)) method. Methods 25 (4), 402–408.

Nagayama, K., Iwamura, Y., Shibata, T., Hirayama, I., Nakamura, T., 2002. Bactericidal activity of phlorotannins from brown alga *Ecklonia kurome*. J. Antimicrob. Chemother. 50, 889–893.

Negara, B., Sohn, J.H., Kim, J.-S., Choi, J., 2021. Effects of phlorotannins on organisms: focus on the safety, toxicity, and availability of phlorotannins. Foods 10 (2), 452.

Pakula, H., Xiang, D., Li, Z., 2017. A tale of two signals: AR and WNT in development and tumorigenesis of prostate and mammary glands. Cancer 9 (12), 14.

Paradis, M.E., Couture, P., Lamarche, B., 2011. A randomized crossover placebo-controlled trial investigating the effect of brown seasweed (*Ascophyllum nodosum* and *Fucus vesiculosus*) on postchallenge plasma glucose and insulin levels in men and women. Appl. Physiol. Nutr. Metabol. 36, 913–919.

Park, S.-J., Min, K.-J., Park, T.-G., 2012. Nutritional characteristics and screening of biological activity of *Agarum cribrosum*. Korean J. Food Nutr. 25 (4), 842–849.

Phasanasophon, K., Kim, S.M., 2017. Antioxidant and cosmeceutical activities of *Agarum cribrosum* phlorotannin extracted by ultrasonication treatment. Nat. Prod. Commun. 13 (5), 565–570.

Phasanasophon, K., Kim, S.M., 2019. Anti-inflammatory activity of the phlorotannin trifuhalol A using LPS-stimulated RAW264.7 cells through NF-κB and MAPK main signaling pathways. Nat. Prod. Commun. 14 (5), 1–8.
Shin, H.C., Kim, S.H., Park, Y., Lee, B.H., Hwang, H.J., 2012. Effects of 12-week oral supplementation of *Ecklonia cava* polyphenols on anthropometric and blood lipid parameters in overweight Korean individuals: a double-blind randomized clinical trial. Phytother Res. 26, 363–368.
Singleton, V.L., Rossi, J.A., 1965. Colorimetry of total phenolics with phosphomolybdic-phosphotungstic acid reagent. Am. J. Enol. Vitic. 16, 144–158.
Song, Q., Wang, J., 2020. Effects of the lignin compound (+)-Guaiacin on hair cell survival by activating Wnt/β-catenin signaling in mouse cochlea. Tissue Cell 66, 101393.
Turch, D., Bresson, J.-L., Burlingame, B., Dean, T., Fairweather-Tai, S., Heinonen, M., Hirsch-Ernst, K., Mangelsdorf, I., McArdle, H., Naska, A., et al., 2017. Safety of *Ecklonia cava* phlorotannins as a novel food pursuant to Regulation (EC) No 258/97. EFSA J. 15, 5003–5018.
Um, M.Y., Kim, J.Y., Hang, J.K., Kim, J., Yang, H., Yoon, M., Kim, J., Kang, S.W., 2018. Phlorotannin supplement decreases wake after sleep onset in adults with self-reported sleep disturbance: a randomized, controlled, double-blind clinical and polysomnographic study. Phytother Res. 32, 698–704.
Ummat, V., Tiwari, B.K., Jaiswal, A.K., Condon, K., Garcia-Vaquero, M., O'Doherty, J., O'Donnell, C., Rajauria, G., 2020. Optimisation of ultrasound frequency, extraction time and solvent for the recovery of polyphenols, phlorotannins and associated antioxidant activity from brown seaweeds. Mar. Drugs 18 (5), 250.
van Tienen, F.H.J., Laeremans, H., van der Kallen, C.J.H., Smeets, H.J.M., 2009. Wnt5b stimulates adipogenesis by activating PPARgamma, and inhibiting the beta-catenin dependent wnt signaling pathway together with Wnt5a. Biochem. Biophys. Res. Commun. 387, 209–211.
Venkatesan, J., Keekan, K.K., Anil, S., Bhatnagar, I., Kim, S.-K., 2019. Phlorotannins. Food Chem. (Oxf). 2019, 515–527.
Wang, F., Zhu, Y., Wang, F., Wang, Y., Dong, B.-J., Wang, N., Gao, W.-Q., 2020. Wnt/β-catenin signaling contributes to prostate cancer heterogeneity through reciprocal suppression of H3K27 trimethylation. Biochem. Biophys. Res. Commun. 527 (1), 242–249.
Ye, Z., Go, G.-W., Singh, R., Liu, W., Keramati, A.R., Mani, A., 2017. LRP6 protein regulates low density lipoprotein (LDL) receptor-mediated LDL uptake. J. Biol. Chem. 287 (2), 1335–1344.
Yoon, J.-Y., Choi, H., Jun, H.-S., 2017. The effect of phloroglucinol, a component of *Ecklonia cava* extract, on hepatic glucose production. Mar. Drugs 15 (4), 106.
Zhang, X., Dong, S., Xu, F., 2018. Structural and druggability landscape of frizzled G protein-coupled receptors. Trends Biochem. Sci. 43 (12), 1033–1046.
Zhao, J., Yue, W., Zhu, M.J., Sreejayan, N., Du, M., 2010. AMP-activated protein kinase (AMPK) cross-talks with canonical Wnt signaling via phosphorylation of beta-catenin at Ser 552. Biochem. Biophys. Res. Commun. 395 (1), 146–151.